

Photoconductivity and infrared absorption study of hydrogen-related shallow donors in ZnO

E. V. Lavrov,* F. Börrnert, and J. Weber

Institute of Applied Physics, TU Dresden, 01062 Dresden, Germany

(Received 26 April 2005; published 15 August 2005)

Vapor phase grown ZnO samples treated with hydrogen and/or deuterium plasma were studied by means of photoconductivity and infrared (IR) absorption spectroscopy. Three bands at 180, 240, and 310 cm^{-1} were observed in the photoconductivity spectra of hydrogenated ZnO. These are identified as electronic transitions of three independent hydrogen-related shallow donors. Two electronic transitions from the H-I defect previously associated with the bond-centered hydrogen [E. V. Lavrov *et al.*, Phys. Rev. B **66**, 165205 (2002)] were found in IR absorption spectra at 1430 and 1480 cm^{-1} . Based on the energies of these transitions H-I was ruled out as a candidate for the hydrogen-related shallow donor in ZnO.

DOI: [10.1103/PhysRevB.72.085212](https://doi.org/10.1103/PhysRevB.72.085212)

PACS number(s): 61.72.Ji, 78.30.Fs

I. INTRODUCTION

Due to unique optical, electronic, and mechanical properties, ZnO is at the moment a subject of extensive studies. Nearly all as-grown ZnO crystals reveal *n*-type conductivity. First-principle calculations indicate that hydrogen in ZnO always occurs in the positive charge state, that is, acts as a donor.¹

This hypothesis has found its experimental confirmation: It was established that hydrogen forms a number of shallow donors in ZnO with ionization energies ranging from 35 to 65 meV.^{2–4} Though hydrogen is not considered a main cause of *n*-type conductivity (for example, see Ref. 5) it strongly affects the electrical activity of the crystal and deeper understanding of its properties in ZnO is needed.

Infrared absorption spectroscopy both on the local vibrational modes (LVMs) and electronic states of hydrogen-related defects seems to be a good tool to address this issue experimentally. Knowledge about LVMs gives detailed insight into the microscopic structure whereas electronic transitions supplies important information about the electrical activity of the defect.

A number of hydrogen-related centers was found and investigated by means of IR absorption spectroscopy.^{6–13} Two of these were suggested as candidates for possible shallow donors in ZnO. The first one labeled H-I was tentatively identified as bond-centered hydrogen with the O–H bond aligned with the *c* axis of the crystal.⁸ At 10 K the center possesses a stretch LVM with a frequency of 3611.3 cm^{-1} . The second defect was identified as hydrogen located at the antibonding site with the O–H bond oriented 112° from the *c* axis.⁹ The LVM frequency of the defect at 10 K was found to be 3326.3 cm^{-1} .

However, the assignment of the defects responsible for the 3611.3 and 3326.3 cm^{-1} lines to shallow donors in ZnO remains speculative since no IR absorption experiments below 600 cm^{-1} were reported, i.e., in the region where according to the effective mass (EM) theory the electronic transitions from shallow donors should take place.

The main difficulty arises from the fact that ZnO is an ionic crystal and because of this its reflectivity in the Reststrahlen band, i.e., between the lowest TO (380 cm^{-1}) and the highest LO phonon modes (590 cm^{-1}), approaches 90%.

Moreover, the absorption coefficient of ZnO below 600 cm^{-1} was found to be at least 100 cm^{-1} .^{14–17} Altogether, this implies that direct IR absorption measurements on shallow donors in ZnO are hardly possible.

Another way to approach this problem is to study photoconductivity (PC) of ZnO. The most relevant modification of this technique for our purposes is called photothermal ionization spectroscopy (PTIS) and consists of two steps: (i) Excitation of an electron from the ground to one of the excited states of a donor by light absorption; and (ii) further excitation of the electron from the excited state to the conduction band by phonon absorption. PTIS is a highly sensitive spectroscopic technique and in Si or Ge can theoretically detect individual concentrations of shallow impurities as low as 10⁷ cm^{-3} (for comprehensive reviews of PTIS see Refs. 18 and 19).

To our knowledge, no PC study on shallow impurities in ZnO has been performed so far. Here we report on the results of combined photoconductivity and IR absorption studies of hydrogen-related shallow donors in ZnO.

II. EXPERIMENTAL DETAILS

The ZnO crystals used in this work were hexagonal prisms with a diameter of about 2 mm and a length of ~20 mm. The nominally undoped *n*-type ZnO single crystals with resistivity of 10–100 Ω cm were grown from the vapor phase at the Institute for Applied Physics, University of Erlangen (Germany).^{20,21}

Hydrogen and/or deuterium was introduced into the samples from a remote dc plasma. The exposure time was 2–19 h and the sample temperature during the treatment was 350–380 °C. A detailed description of our plasma system is given elsewhere.⁸

In order to study the annealing behavior of the defects discussed in this work, ZnO samples were exposed to isochronal heat treatments (anneals) at temperatures in the range of 150–800 °C. The anneals were performed in a furnace purged with argon gas and the duration of each treatment was 30 min.

For photoconductivity measurements the ZnO samples were etched with ortho-phosphoric acid for one minute at

room temperature then ohmic contacts were scratched with a mixture of In-Ga. The contacts were approximately 1 cm apart with an area of $2 \times 2 \text{ mm}^2$ and were located on the illuminated face of a sample.

Photoconductivity and infrared absorption spectra were recorded with a BOMEM DA3.01 Fourier transform spectrometer equipped with a globar light source, a KBr or mylar (3 or 6 μm thick) beamsplitter, and a liquid-nitrogen-cooled mercury cadmium telluride (MCT) detector, or liquid-helium-cooled Si:B detector. The choice of beamsplitter/detector depended on the spectral range desired. With the appropriate configuration, the frequency range from 100 to 6000 cm^{-1} could be covered. The spectral resolution was 1 to 2 cm^{-1} .

The samples were positioned in an exchange-gas cryostat equipped either with polypropylene or ZnSe windows. The temperature was stabilized within 1 K in the range 9–30 K. A platinum resistor was used as a thermometer. Polarized light was produced by putting a wire-grid polarizer with a KRS-5 substrate in front of the cryostat.

III. SHALLOW DONORS IN ZnO

ZnO crystallizes in a wurtzite type lattice. The effective mass of an electron in the conduction band is isotropic $m^* = 0.275m_e$, but the static dielectric constant is a tensor with the main values of $\epsilon_{\parallel} = 8.75$ and $\epsilon_{\perp} = 7.8$.²² Here indices “ \parallel ” and “ \perp ” denote the directions parallel and perpendicular to the c axis of the crystal, respectively.

The effective-mass Hamiltonian for the donor electron at the zone center in a uniaxial crystal with the c axis along the z direction, is given by

$$H = -\frac{\hbar^2}{2m^*}\Delta - \frac{e^2}{\sqrt{\epsilon_{\parallel}\epsilon_{\perp}(x^2 + y^2 + \epsilon_{\perp}z^2/\epsilon_{\parallel})}}. \quad (1)$$

If the values of ϵ_{\parallel} and ϵ_{\perp} are close to each other, one can use the perturbation theory in order to find the energy values and wave functions of the shallow donor in wurtzite semiconductors.²³ The donor energy levels in ZnO obtained in this way are

$$\begin{aligned} E_{ns} &= -E_n(1 + \alpha/3) \\ E_{np_z} &= -E_n(1 + 3\alpha/5) \\ E_{np_x} = E_{np_y} &= -E_n(1 + \alpha/5), \end{aligned} \quad (2)$$

where $\alpha = (\epsilon_{\parallel} - \epsilon_{\perp})/\epsilon_{\parallel}$ and

$$E_n = \frac{m^*}{\epsilon_{\parallel}\epsilon_{\perp}m_e} \frac{13.6 \text{ eV}}{n^2} = \frac{55 \text{ meV}}{n^2}.$$

Here, as usual, n is the principal quantum number and s, p denote the states with the orbital momentum of 0 and 1, respectively.

Due to selection rules the dominant transitions in IR absorption and photoconductivity spectra are those from the ground $1s$ to the excited p states. In Table I we give the energies of the first six dipole allowed transitions for an EM

TABLE I. Energies of the dipole allowed transitions for an EM shallow donor in ZnO calculated from Eq. (2).

| Transition | Energy (cm^{-1}) |
|------------------------------------|-----------------------------|
| $1s \rightarrow 2p_z$ | 340 |
| $1s \rightarrow 2p_{x,y}$ | 345 |
| $1s \rightarrow 3p_z$ | 406 |
| $1s \rightarrow 3p_{x,y}$ | 408 |
| $1s \rightarrow 4p_z$ | 429 |
| $1s \rightarrow 4p_{x,y}$ | 430 |
| $1s \rightarrow \text{Cond. band}$ | 458 |

shallow donor in ZnO. The main uncertainty of these values comes from the not well known ϵ and m^* .

Further complication of a simple hydrogenic model for a spherical shallow donor results from the deviation of the actual potential from that of the Coulomb one at $r \leq a_0$, where a_0 is the lattice constant. The most pronounced effect it has on the ground s state of the donor due to nonzero value of the wave function at $r=0$. That is, the ground state energy shifts as compared to the predictions of the EM theory. This shift is called chemical or central cell correction. The excited states, however, remain nearly unchanged. Based on this we expect that the splittings between the p_z and $p_{x,y}$ states given in Table I are relevant for a real donor even though the absolute value is most likely not.

The value of the chemical shift in direct-gap semiconductors is of the order of magnitude of $\epsilon E_i (a_0/a)^2$, where a is the effective Bohr radius of the impurity and E_i is the ionization energy determined from the EM theory.¹⁸

In ZnO this quantity is about 30 meV, i.e., the ionization energies of shallow donors in ZnO should range from 40 to 70 meV. Experimental values of E_i in ZnO were found to be between 35 and 65 meV.²⁻⁴

IV. PHOTOCONDUCTIVITY

A. General properties of the PC spectra

Our virgin ZnO samples reveal no PC signal. The bottom spectrum in Fig. 1 shows a typical PC signal of a ZnO sample after hydrogenation. The bars in the figure mark the expected transitions of an ideal EM shallow donor in ZnO (see Table I).

The top spectrum in Fig. 1 shows the reflectivity of ZnO. The dots are experimental values taken from Ref. 14. Since no data for reflectivity of ZnO below 250 cm^{-1} are available in the literature the experimental points were fitted by the classical theory of dispersion (solid line in the top spectrum).²⁴

The best fit was obtained with $\epsilon_0 = 3.7$, $\epsilon_{\infty} = 7.8$, $\Omega_0 = 402 \text{ cm}^{-1}$, and $\gamma = 0.033$. Here, ϵ_0 and ϵ_{∞} are the static and high frequency dielectric constants, respectively; Ω_0 is the resonance frequency of the oscillator; and γ is the damping constant. For the sake of simplicity we assumed that the dielectric constant is isotropic. Note that the fitting parameters ϵ_0 , ϵ_{∞} , and Ω_0 are in reasonable agreement with those

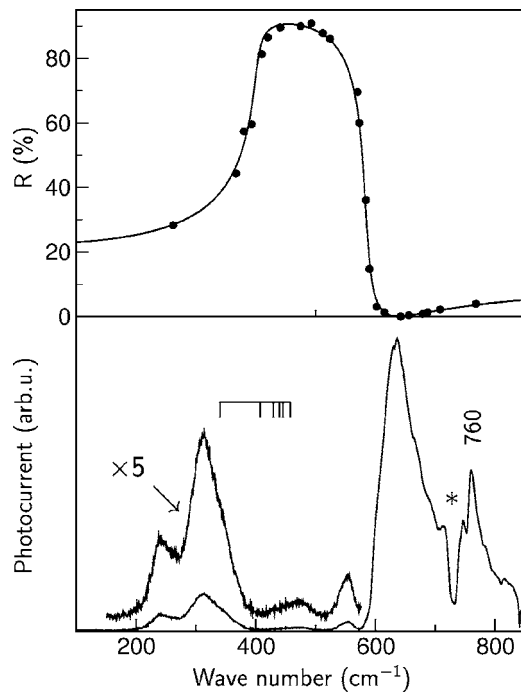


FIG. 1. Bottom—section of photoconductivity spectrum measured at 14 K for a ZnO sample treated with a hydrogen plasma at 350 °C for 2 h. $\mathbf{k} \perp c$. Unpolarized light. Top—reflectivity of ZnO: Dots—experimental values from Ref. 14; solid line—fit from the classical theory of dispersion (see text). The dip marked “*” is an artefact originating from the mylar beamsplitter of the spectrometer and the cryostat windows.

known from the literature.²² Here, the resonance frequency of the oscillator should be compared to the frequency of the zone-centered TO phonon.

From comparison of the two spectra in the figure we see that the gap in the PC intensity spans from about 400 to 600 cm^{-1} and correlates very well with the highest reflectivity of ZnO (the Reststrahlen band). We take this as an indication that the PC signal originates from the bulk rather than from the surface of the sample. Note that most of the transitions from the EM shallow donor fall into the Reststrahlen band.

Since, to our knowledge, no photoconductivity studies of ZnO below 1000 cm^{-1} have been reported in the literature there is a need to give a general description of the PC spectra before we come to the discussion of hydrogen-related shallow donors in ZnO.

The bottom spectrum in Fig. 2 shows a PC signal of a hydrogenated ZnO sample at frequencies not given in the previous figure. A number of features at 760, 830, 960, and 1060 cm^{-1} is clearly seen in the spectrum. In order to elucidate their origin we recorded a transmission spectrum of a virgin ZnO sample given in the top of Fig. 2. Interestingly, ZnO is transparent for the light only at frequencies marked in the figure. That is, the features at 760, 830, 960, and 1060 cm^{-1} are seen both in PC and transmission spectra. Further investigation has shown that these are Fano resonances²⁵ and are detected for any ZnO available in our group. The detailed study of the 760, 830, 960, and

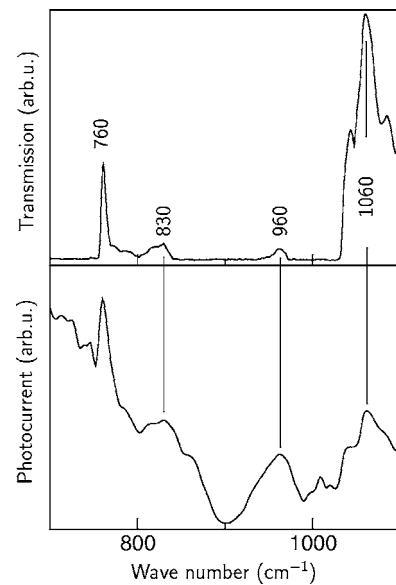


FIG. 2. Bottom—section of photoconductivity spectrum measured at 19 K for a ZnO sample treated with an H+D plasma at 380 °C for 19 h. Top—section of transmission spectra measured at 10 K for a virgin ZnO sample. $\mathbf{k} \perp c$. Unpolarized light.

1060 cm^{-1} bands is beyond the scope of this paper and will be addressed in the future communication. Here it is important that these features are not related to hydrogen and their presence in the PC spectra only implies that due to higher transmission at the appropriate frequencies the effective probing depth of the ZnO sample is proportionally enhanced.

The bottom spectrum in Fig. 3 shows the PC signal of hydrogenated ZnO in the Reststrahlen region. For comparison, in the top of the figure we give an absorption coefficient, α , of ZnO calculated from the classical theory of dispersion with the same parameters used to fit the reflectivity of ZnO (see Fig. 1). As expected, the strongest absorption ($\alpha \approx 4.5 \times 10^4 \text{ cm}^{-1}$) occurs at 405 cm^{-1} , that is, close to the reso-

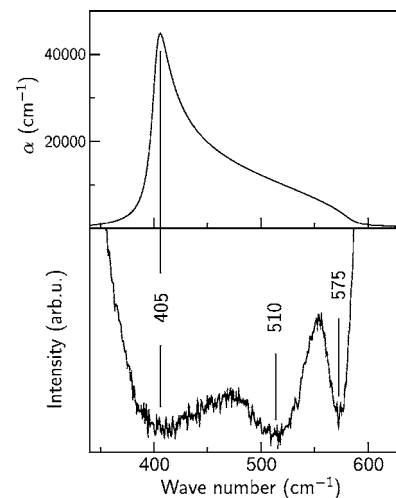


FIG. 3. Bottom—section of photoconductivity spectrum in the Reststrahlen region (the same as in Fig. 1). Top—absorption coefficient of ZnO calculated from the classical theory of dispersion (see text).

TABLE II. Dependency of the free carriers concentration (electrons) at room temperature in VP-grown ZnO in the course of hydrogen plasma treatment and subsequent anneal (for details see text).

| Treatment | R (Ω) | n (cm^{-3}) |
|---------------|----------------|--------------------------|
| Virgin | 1000 | 8×10^{14} |
| H-plasma | 100 | 8×10^{15} |
| 430 °C anneal | 240 | 3×10^{15} |
| 800 °C anneal | 640 | 10^{15} |

nance frequency of the oscillator $\Omega_0 = 402 \text{ cm}^{-1}$. No signal in photoconductivity spectra can be observed around Ω_0 , which gives further support to our assignment of the PC signals as those originating from the bulk rather than from the surface of the sample.

The other two minima in the PC spectrum occur at 510 and 575 cm^{-1} and do not depend on the details of the sample preparation, such as plasma parameters, starting material, or annealing temperature. Based on this we suggest that the dips in the PC spectra at 510 and 575 cm^{-1} originate from two-phonon absorption of different lattice phonons.

B. Temperature stability of the PC lines

The concentration of free carriers n can be estimated from

$$R = \rho \frac{l}{S}, \quad \rho^{-1} = en\mu. \quad (3)$$

Here, R is the resistance, l is the distance between the contacts, S is the cross section of the sample, ρ is the resistivity, e is the elementary charge, and μ is the mobility. Since our samples always reveal n -type conductivity, from the above relations we may obtain the concentration of free electrons in the conduction band.

The electron mobility of ZnO samples similar to those employed in this study was $\mu \approx 200 \text{ cm}^2 \text{ V}^{-1} \text{ s}^{-1}$ (see Ref. 26), $l \approx 1 \text{ cm}$, and $S \approx 2 \times 2 \text{ mm}^2$. A typical resistance R of our as-received ZnO samples was around $1 \text{ k}\Omega$. With these values we find that the concentration of free electrons in the virgin material at room temperature is around 10^{15} cm^{-3} . As mentioned before, our virgin ZnO samples do not reveal any noticeable PC signal.

After the hydrogenation in a plasma at $350 \text{ }^\circ\text{C}$ for 2 h the resistance of ZnO drops by an order of magnitude, which corresponds to $n \approx 10^{16} \text{ cm}^{-3}$ (see Table II). This strongly indicates that hydrogen results in the formation of shallow donors in ZnO.

According to the EM model, the shallow donors in ZnO should give rise to a PC signal below 600 cm^{-1} . Figure 4 provides a spectroscopic evidence for the formation of shallow donors in ZnO. Three broad bands at 180, 240, and 310 cm^{-1} with full width at half maximum (FWHM) around 50 cm^{-1} appear in a photoconductivity spectrum of the as-treated sample. The relative intensities of these lines strongly depend on the details of sample preparation, which implies that they belong at least to three different shallow donors.

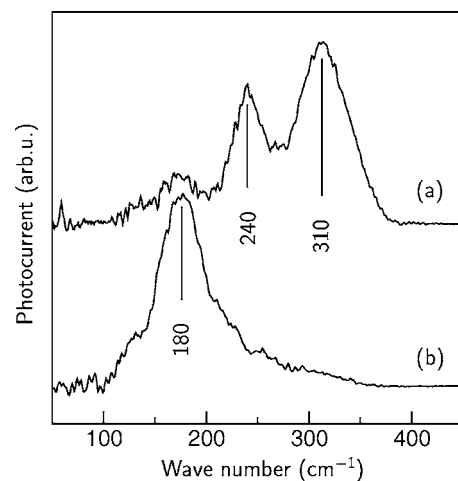


FIG. 4. Sections of photoconductivity spectra measured at 14 K for a ZnO sample treated with a hydrogen plasma at $350 \text{ }^\circ\text{C}$ for 2 h. Top—as-treated, bottom—after anneal at $430 \text{ }^\circ\text{C}$ for 30 min.

Subsequent anneal of the hydrogenated ZnO at $430 \text{ }^\circ\text{C}$ results in the decrease of the free carriers concentration to approximately $3 \times 10^{15} \text{ cm}^{-3}$. Spectroscopically, this treatment considerably weakens the bands at 240 and 310 cm^{-1} , whereas the 180 cm^{-1} line becomes a dominant signal in the PC spectrum (see Fig. 4).

It is well-known that high temperature heat treatment drives most of hydrogen out of ZnO. Indeed, the anneal at $800 \text{ }^\circ\text{C}$ nearly recovers the original resistivity of the ZnO sample (see Table II) and no PC signal could be obtained afterwards. This finding gives further support for the assignment of the 180, 240, and 310 cm^{-1} lines as those originating from the hydrogen-related shallow donors in ZnO.

C. Isotope effect on the PC spectra

Normally, the dependency of electronic transitions from the isotope substitution comes from the dependency of the zero-point energy on the isotope mass. In Si, for example, the electronic transitions of hydrogen-related shallow donors shift towards higher energies by $\sim 0.1 \text{ cm}^{-1}$ when hydrogen is replaced by deuterium.²⁷

The effect of isotope substitution on the PC signals in ZnO is presented in Fig. 5. The figure shows two spectra obtained after hydrogen or deuterium plasma treatment of ZnO samples at $350 \text{ }^\circ\text{C}$.

It follows from the figure that within the accuracy of our setup the 180 cm^{-1} line seems to be independent of the hydrogen isotope, whereas the 240 and 310 cm^{-1} lines experience a “red” shift towards 235 and 300 cm^{-1} , respectively, when hydrogen is replaced by deuterium. That is, as compared to Si, the frequency shift has an opposite sign and is more than one order of magnitude stronger.

Though qualitative influence of the hydrogen isotope on the photoconductivity spectra is there, the quantitative analysis of the isotope effect is difficult. The 310 and 240 cm^{-1} bands are positioned at the steep edge of the strong absorption band of the ZnO crystal (see Fig. 3). Since all the PC signals are fairly broad and overlap significantly, the latter

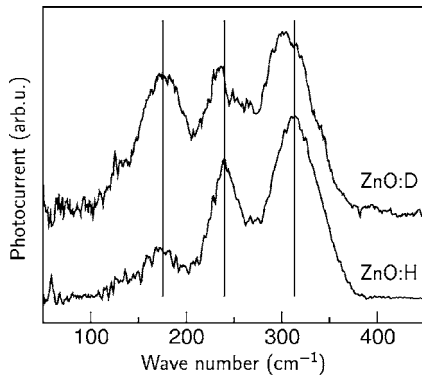


FIG. 5. Sections of photoconductivity spectra measured at 14 K for a ZnO sample treated with a hydrogen (bottom) and deuterium (top) plasmas at 350 °C for 2 h.

circumstance implies that the apparent shapes of the 240 and 310 cm^{-1} bands seen in the spectra are distorted as compared to the “perfect” ones. This, in turn, suggests that the actual isotope shift of the PC bands might considerably deviate from the PC peak shifts seen in the spectra.

Nevertheless, the obvious difference between the hydrogen and deuterium cases is also in favor of the model of 240 and 310 cm^{-1} bands as electronic transitions from the hydrogen-related shallow donors in ZnO.

V. IR ABSORPTION

An important question concerns the microscopic nature of hydrogen-related shallow donors in ZnO. Two candidates have been proposed so far. The first one, labeled as H-I, was tentatively identified as bond-centered hydrogen with the O–H bond aligned with the c axis of the crystal.⁸ At 10 K the defect has a stretch local vibrational mode with a frequency of 3611.3 cm^{-1} . The second defect was assigned to hydrogen located at the antibonding site of the lattice with the O–H bond oriented 112° from the c axis.⁹ At 10 K the defect possesses a stretch mode at 3326.3 cm^{-1} . Since the 3326.3 cm^{-1} line was never observed in our samples, it cannot be responsible for the 180, 240, and 310 cm^{-1} lines in the photoconductivity spectra.

The H-I defect, however, is always present in our ZnO samples after hydrogenation. Therefore, we revisited this assignment in order to find out if there is any correlation between H-I and any other electronic transition. No line in the PC spectra was found which could be unambiguously associated with this defect. Careful inspection of the IR absorption spectra revealed, however, two extra lines which are related to the H-I signal. These are shown in Fig. 6.

The IR absorption of the virgin ZnO is shown in Fig. 6(a). As usual, no H-I signal is present. It follows also from the figure that the spectra reveal two lines at 1415 and 1446 cm^{-1} the origin of which is not clear at the moment.

Figure 6(b) shows the effect of plasma treatment on a ZnO sample. The hydrogenation results in formation of H-I, whereas the 1415 and 1446 cm^{-1} lines become much weaker. Not shown in the figure is the signal from the Zn vacancy passivated with two hydrogen atoms, $V_{\text{Zn}}\text{H}_2$ (the 3312.2 and

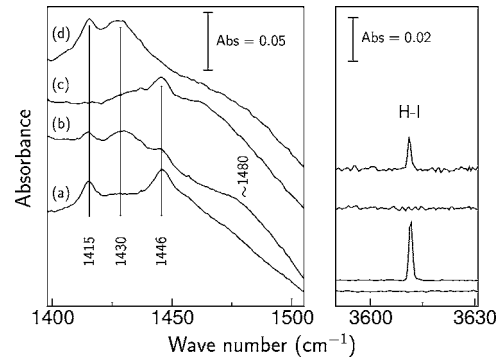


FIG. 6. Sections of IR absorption spectra of ZnO sample treated with H plasma: (a) Virgin sample, unpolarized light; as-treated sample (b) unpolarized light, (c) $\mathbf{E} \perp c$, (d) $\mathbf{E} \parallel c$. $\mathbf{k} \perp c$.

3349.6 cm^{-1} lines), which also appears in the IR absorption spectra after hydrogenation.⁸ $V_{\text{Zn}}\text{H}_2$ anneals out in the course of subsequent heat treatments while the 1415 and 1446 cm^{-1} lines recover the original intensity. However, the anticorrelation between these lines and $V_{\text{Zn}}\text{H}_2$ is not perfect so that the 1415 and 1446 cm^{-1} cannot be directly assigned to the electronic transitions of the Zn vacancy.

From Fig. 6(b) we also see that hydrogenation results in formation of two previously not reported IR absorption lines positioned at 1430 and 1480 cm^{-1} . Of these two, the line at ~ 1480 is much broader which makes the investigation of its properties a hard task. Nevertheless, the signal is real.

It follows from Figs. 6(c) and 6(d) spectra that the polarization properties of the 1430 cm^{-1} line are identical to those of H-I. That is, the 1430 cm^{-1} line is polarized with the c axis of the crystal.

The assignment of the 1430 cm^{-1} line can be done on the basis of its temperature stability presented in Fig. 7. Here the normalized intensities of the 1430 and 3611.3 cm^{-1} lines as a function of the annealing temperature are shown. Obviously, the two signals reveal identical behavior and we conclude that the 1430 cm^{-1} transition belongs to H-I. Due to high FWHM of the 1480 cm^{-1} line we could not investigate its temperature stability quantitatively. Nevertheless, because the 1480 cm^{-1} line always accompanies the 3611.3 cm^{-1} one in the IR absorption spectra we also assigned it to the H-I defect.

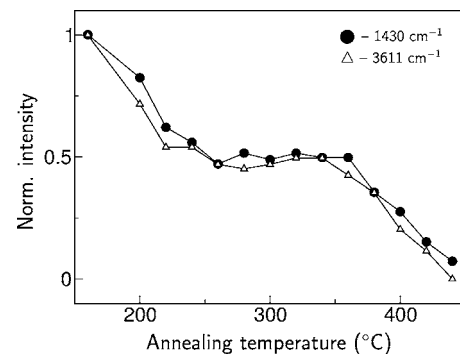


FIG. 7. Annealing behavior of the 1430 and 3611 cm^{-1} IR absorption lines. The intensities were measured at 10 K for a ZnO sample treated with H-plasma at 350 °C for 4 h.

One more conclusion can be drawn from Fig. 7. The first annealing step at 200 °C results in a considerable drop of the H-I intensity even though the hydrogenation took place at 350 °C. This indicates that the apparent annealing behavior of H-I is determined by the recapture/diffusion of hydrogen and the dissociation of H-I occurs at much lower temperature than 400 °C. This, in turn, provides further support for the model of H-I as a bond-centered hydrogen, since the diffusion barrier, ΔE , of isolated H in ZnO was found to be about 0.9–1.1 eV.^{28,29} Note that recent SIMS data suggest much smaller value of ΔE that is equal to 0.17 ± 0.12 eV.³⁰

The nature of the 1430 and 1480 cm^{-1} transitions could be elucidated from the isotope substitution experiments. No noticeable shift was found for these lines when hydrogen was replaced by deuterium. This implies that these are electronic transitions of H-I rather than hydrogen-related local vibrational modes. The energies of these transitions (177 and 184 meV) lead us to the conclusion that the H-I defect cannot be associated with a shallow donor and should be assigned to a deep defect. Combined IR absorption and deep level transient spectroscopy studies are needed to find out if the H-I defect has a deep level in the band gap.

VI. DISCUSSION

A typical PC spectrum of a shallow impurity consists of a set of sharp lines with frequencies below ionization energy E_i and a broad band at $\hbar\omega > E_i$. The broad band intensity rises very steeply at frequencies close to E_i and falls as $\omega^{-3.5}$ well above E_i .³¹ It characterizes the transitions from the ground state of the impurity to the conduction/valence band. The sharp lines of the PC spectrum are transitions from the ground to the excited states of the defect.¹⁸

The highest reported ionization energy of hydrogen-related shallow donor in ZnO is 65 meV (524 cm^{-1}).³ Based on this we assign the PC signal above 524 cm^{-1} to the direct transitions from the ground state of the shallow donors to the conduction band.

The lowest reported ionization energy in ZnO for hydrogen-related shallow donors was 35 meV (282 cm^{-1}).³ This leads us to suggestion that the 180 and 240 cm^{-1} bands in the PC spectra are transitions from the ground to the excited states of two shallow donors in ZnO.

The nature of the 310 cm^{-1} (38 meV) band is much more difficult to elucidate since its frequency may in principle fit both the ionization energy and an internal transition of a shallow donor in ZnO. In some samples we found this line to be the only “sharp” signal in the PC spectra with FWHM of “only” 30 cm^{-1} . Based on this finding the 310 cm^{-1} band should be assigned to another hydrogen-related shallow donor different from those giving rise to the 180 and 240 cm^{-1} lines. No further assignment for this line can be given at the moment.

If we assume that the 180 and 240 cm^{-1} bands are internal transitions rather than transitions from the ground state of two independent hydrogen-related shallow donors to the conduction band these lines should be the $1s \rightarrow 2p$ transitions. Normally, because of the strongest oscillator strength it is this transition that dominates the PC spectra from a shallow impurity.^{18,32}

TABLE III. Ionization energies for hydrogen-related shallow donors in ZnO observed in Fig. 4.

| Donor | PC line (cm^{-1}) | Assignment | E_i (meV) |
|-------|------------------------------|---------------------|-------------|
| SDI | 180 | $1s \rightarrow 2p$ | 37 |
| SDII | 240 | $1s \rightarrow 2p$ | 44 |
| SDIII | 310 | ? | ≥ 38 |

With this assumption one can estimate the ionization energies of shallow donors SDI and SDII responsible for the 180 and 240 cm^{-1} lines in the PC spectra. These values are summarized in Table III. For these estimates we assumed that the chemical shift has an effect only on the ground $1s$ state of the donor whereas the positions of the excited levels with respect to the ionization energy remain unchanged and can be obtained from Eq. (2).

It follows from the table that the ionization energy of the SDI donor matches fairly well the ionization energy of the shallow donor studied by means of electron paramagnetic resonance and Hall measurements.³ The second shallow donor labeled as SDII fits reasonable well the ionization energy of the shallow donor responsible for the photoluminescence line at 3.363 eV and labeled as I_4 . From the two electron satellite transition in the PL spectra the ionization energy of I_4 was estimated to be 47 meV.⁴

The high FWHM of the 180, 240, and 310 cm^{-1} lines makes further analysis of the PC signals meaningless. We consider the following reasons which may result in broadening of PC transitions. These are high concentration of: (i) Shallow donors; (ii) compensating acceptors; and (iii) residual isoelectronic impurities.

The linewidth of the spectral lines is often determined by the interaction of the impurity centers. The two nearby impurities in the neutral state couple through the dipole-dipole force. The broadening of the excited states due to the interaction of the excited atom with another one being in the ground state is of order $E_i(a/R)^3$, where a is the Bohr radius ($R \gg a$) and R is the mean distance between the impurities.¹⁸

As follows from Table II, the highest concentration of shallow donors in our ZnO samples is about 10^{16} cm^{-3} . In this case the broadening of the PC lines due to the interaction of the nearby shallow donors in ZnO is of the order 0.01 cm^{-1} , which, apparently cannot explain the experimental value of $\sim 50 \text{ cm}^{-1}$.

If additionally to shallow donors our ZnO samples contain acceptors as compensating impurity, the random electric fields of the ionized acceptors will result in additional broadening due to the Stark splitting of the p states. This effect can be estimated from

$$\Delta E \approx 2.6 \times 10^3 E_i (N_A a^3)^{4/3}, \quad (4)$$

where N_A is the acceptor concentration.¹⁸

From Eq. (4) we can estimate the acceptor concentration needed to account for the experimentally observed linewidths of the PC signals. With $E_i = 55 \text{ meV}$, $\Delta E = 50 \text{ cm}^{-1}$, and $a = 13 \text{ \AA}$ we obtain that $N_A = 3 \times 10^{17} \text{ cm}^{-3}$. On the other hand, the concentration of free electrons in the virgin ZnO

samples at room temperature is a factor of 300 less (see Table II) implying nearly perfect degree of compensation. Though this situation is possible we find it very unlikely and believe that high acceptor concentration cannot be the main reason resulting in broadening PC lines.

Besides donors and acceptors some electrically inactive defect complexes are always present in a semiconductor which do not give rise to any level in the band gap. The concentration of such defects may be very large and many times greater than that of the shallow donors. The most important for the broadening is the effect of formation of the complex donor+electrically inactive impurity. The ground state energy of such a complex changes as compared to the ground state energy of the isolated donor due to the change in the chemical shift. The broadening can be roughly estimated to be of the order of $e^2 a_0^2 N$, where e is the elementary charge, a_0 is the lattice parameter, and N is the concentration of the electrically inactive impurities.³³ From here the concentration of electrically inactive impurities needed to explain the broadening of $\sim 50 \text{ cm}^{-1}$ is around $3 \times 10^{19} \text{ cm}^{-3}$.

Taking into account the quality of ZnO available now and the rudeness of this estimate we believe that electrically inactive defects in ZnO can result in large linewidths of the PC lines. Our ZnO sample, of course, contain impurities, but the qualitative information is scarce. Therefore a particular choice is difficult. One possibility could be the damage brought in by the energetic protons during the plasma treatment. An-

other possibility to be considered is hydrogen itself since it does form electrically inactive defects in our ZnO samples, such as Zn vacancy passivated with two hydrogen atoms, $V_{\text{Zn}}\text{H}_2$.⁸ One more candidate might be interstitial H^2 , which is thought to be present in ZnO in great amounts.¹¹

VII. CONCLUSIONS

We presented the results of combined photoconductivity and IR absorption studies on the hydrogen-related shallow donors in ZnO. Three lines at 180, 240, and 310 cm^{-1} have been observed in the photoconductivity spectra. The 180 and 240 cm^{-1} bands were tentatively identified as transistons from the ground to the first excited state of two independent hydrogen-related shallow donors. Two electronic transitions from the H-I defect previously associated with the bond-centered hydrogen were found in the IR absorption spectra at 1430 and 1480 cm^{-1} . Based on the energies of these transitions H-I was assigned to a deep donor.

ACKNOWLEDGMENTS

The authors gratefully acknowledge R. Helbig for supplying the vapor phase grown ZnO samples. E.V.L. acknowledges the Russian Foundation for Basic Research (Grant No. 02-02-16030).

*Also at Institute of Radio-engineering and Electronics, Mokhovaya 11, 101999 Moscow, Russia. Electronic address: edward.lavrov@physik.phy.tu-dresden.de

¹C. G. Van de Walle, Phys. Rev. Lett. **85**, 1012 (2000).

²S. F. J. Cox, E. A. Davis, S. P. Cottrell, P. J. C. King, J. S. Lord, J. M. Gil, H. V. Alberto, R. C. Vilão, J. P. PirottoDuarte, N. Ayres de Campos, A. Weidinger, R. L. Lichti, and S. J. C. Irvine, Phys. Rev. Lett. **86**, 2601 (2001).

³D. M. Hofmann, A. Hofstaetter, F. Leiter, H. Zhou, F. Henecker, B. K. Meyer, S. B. Orlinskii, J. Schmidt, and P. G. Baranov, Phys. Rev. Lett. **88**, 045504 (2002).

⁴A. Schildknecht, R. Sauer, K. Thonke, Physica B **340-342**, 205 (2003).

⁵D. C. Look, C. Coskin, B. Clafin, and G. G. Farlow, Physica B **340-342**, 32 (2003).

⁶F. G. Gärtner and E. Mollwo, Phys. Status Solidi B **89**, 381 (1978).

⁷F. G. Gärtner and E. Mollwo, Phys. Status Solidi B **90**, 33 (1978).

⁸E. V. Lavrov, J. Weber, F. Börrnert, C. G. Van de Walle, and R. Helbig, Phys. Rev. B **66**, 165205 (2002).

⁹M. D. McCluskey, S. J. Jokela, K. K. Zhuravlev, P. J. Simpson, and K. G. Lynn, Appl. Phys. Lett. **81**, 3807 (2002).

¹⁰E. V. Lavrov, Physica B **340-342**, 195 (2003).

¹¹G. A. Shi, M. Saboktakin, M. Stavola, and S. J. Pearton, Appl. Phys. Lett. **85**, 5601 (2004).

¹²L. E. Halliburton, L. Wang, L. Bai, N. Y. Garces, N. C. Giles, M. J. Callahan, and B. Wang, J. Appl. Phys. **96**, 7168 (2004).

¹³E. V. Lavrov, F. Börrnert, and J. Weber, Phys. Rev. B **71**, 035205 (2005).

¹⁴R. J. Collins and D. A. Kleinman, J. Phys. Chem. Solids **11**, 190 (1959).

¹⁵G. Heiland and H. Lüth, Solid State Commun. **5**, 199 (1967).

¹⁶S. Perkowitz, R. K. Murty-Gutta, and A. K. Garrison, Solid State Commun. **9**, 2251 (1971).

¹⁷H. Finkenrath, K. Krug, and N. Uhle, Phys. Status Solidi B **78**, K27 (1976).

¹⁸Sh. M. Kogan and T. M. Lifshits, Phys. Status Solidi A **39**, 11 (1977).

¹⁹T. M. Lifshits, Instrum. Exp. Tech. **36**, 1 (1993).

²⁰G. Müller and R. Helbig, J. Phys. Chem. Solids **32**, 1971 (1971).

²¹R. Helbig, J. Cryst. Growth **15**, 25 (1972).

²²O. Madelung, *Semiconductors: Data Handbook* (Springer-Verlag, Berlin, Heidelberg, New York, 2004).

²³C. H. Henry and K. Nassau, Phys. Rev. B **2**, 997 (1970).

²⁴T. S. Moss, G. J. Burrell, and B. Ellis, *Semiconductor Optoelectronics* (Butterworth, Washington, D.C., 1973).

²⁵E. Janzén, G. Grossmann, R. Stedman, and H. G. Grimmeiss, Phys. Rev. B **31**, 8000 (1985).

²⁶R. Helbig, Ph.D. thesis, University of Erlangen-Nürnberg, Germany, 1970.

²⁷J. Hartung and J. Weber, Phys. Rev. B **48**, 14161 (1993).

²⁸E. Mollwo, Z. Phys. **138**, 478 (1954).

²⁹D. G. Thomas and J. J. Lander, J. Chem. Phys. **25**, 1136 (1956).

³⁰K. Ip, M. E. Overberg, Y. W. Heo, D. P. Norton, S. J. Pearton, C. E. Stutz, B. Luo, F. Ren, D. C. Look, J. M. Zavada, Appl. Phys.

Lett. **82**, 385 (2003).

³¹N. Y. Fan, Rep. Prog. Phys. **19**, 107 (1956).

³²S. M. Myers, M. I. Baskes, H. K. Birnbaum, J. W. Corbett, G. G. DeLeo, S. K. Estreicher, E. E. Haller, P. Jena, N. M. Johnson, R. Kirchheim, S. J. Pearton, and M. J. Stavola, Rev. Mod. Phys.

64, 559 (1992).

³³S. N. Artemenko, A. A. Kal'fa, S. M. Kogan, and V. I. Sidorov, Fiz. Tekh. Poluprovodn. (S.-Peterburg) **8**, 2164 (1974) [Sov. Phys. Semicond. **8**, 1405 (1975)].